Implementation of the MMG library in the Kratos Multiphysics (*AKA Kratos*) framework

MMG Day 2018

Vicente Mataix Ferrándiz [1]   Riccardo Rossi [1]   Eugenio Oñate Ibañez de Navarra [1]

vmataix@cimne.upc.edu

[1] CIMNE. International Center for Numerical Methods in Engineering, Technical University of Catalonia (UPC). Barcelona. Spain

January 17, 2018

Overview

Section 1

Introduction

Objectives

The main aim of this work is to integrate into *MMG* API on the *Kratos* framework

Kratos

Kratos is a framework for building multi-disciplinary finite element programs.

Features

- **KERNEL**: The kernel and application approach is used to reduce the possible conflicts arising between developers of different fields.
- **OBJECT ORIENTED**: The modular design, hierarchy and abstraction of these approaches fits to the generality, flexibility and re-usability required for the current and future challenges in numerical methods. The main code is developed in *C++* and the *Python* language is used for scripting
- **OPEN SOURCE**: The *BSD (Berkeley Software Distribution)* licence allows to use and distribute the existing code without any restriction, but with the possibility to develop new parts of the code on an open or close basis depending on the developers.
- **FREE**: Because is devoted mainly to developers, researchers and students and, therefore, is the most fruitful way to share knowledge and built a robust numerical methods laboratory adapted to their users' needs. Please, read the license for more detailed information.

Kratos structure classes

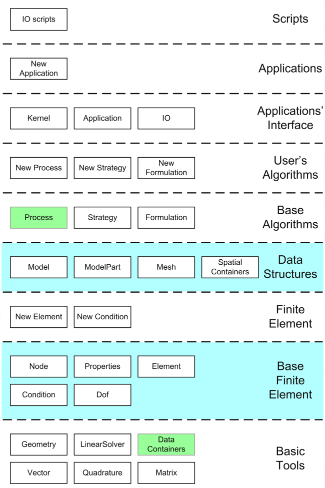

Figure 1: Kratos structure classes

Groups

- *Scripts:* Simple scripted programs created in order to reduce the workload and simplify run problems
- *Applications:* This is the base of the modularity of **Kratos**. Each application can be defined o solve an specific problem and couple them later
- *App interface (core):* Communicate each components and define the framework behaviour
- *Algorithms:* Operations that are used to solve the problem (strategies, time schemes, algorithms, etc...)
- *Data structure:* Contains the information of the problem (geometries, elements, etc...)
- *Finite element:* The base components necessaries to define a **FE** problem (DoF, elements, nodes, etc...)
- *Basic tools:* Algebraic and mathematic components

The groups and classes in **cyan** and **green** will be detailed later for being more related with the *Kratos-MMG* integration

Data structures classes

Model

Model stores the whole model to be analyzed. All Nodes, Properties, Elements, Conditions and solution data

ModelPart

ModelPart holds all data related to an arbitrary part of model. It stores all existing components and data like Nodes, Properties, Elements, Conditions and solution data related to a part of model

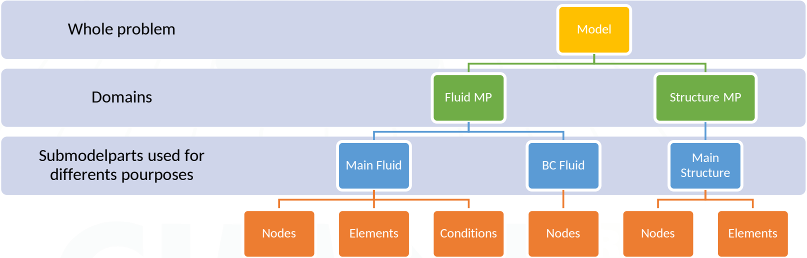

Figure 2: Example

Finite element classes

`Node`

`Node` It is a point with additional facilities. Stores the nodal data, historical nodal data, and list of *DoF*

`Condition`

`Condition` encapsulates data and operations necessary for calculating the local contributions of `Condition` to the global system of equations. *Neumann* conditions are example

`Elements`

`Element` encapsulates the elemental formulation in one object and provides an interface for calculating the local matrices and vectors necessary for assembling the global system of equations. It holds its geometry that meanwhile is its array of `Nodes`. Also stores the elemental data

`Properties`

`Properties` encapsulates data shared by different `Elements` or `Conditions`. It can store any type of data

`DoF`

`DoF` represents a degree of freedom (*DoF*). This class enables the system to work with different set of *DoFs* and also represents the *Dirichlet* condition assigned to each *DoF*

Colours identification

In in our implementations we use a processes to set the **BC** (both *Neumann* or *Dirichlet*)

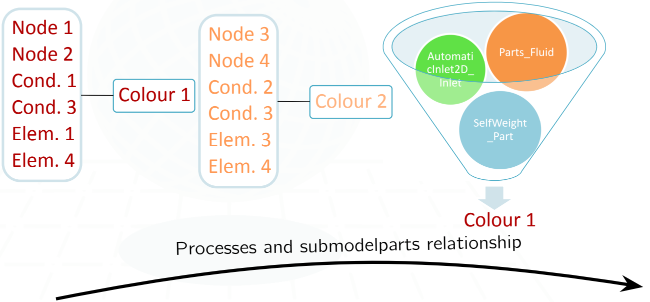


```
"python_module" : "apply_inlet_process",
"kratos_module" : "KratosMultiphysics.FluidDynamicsApplication",
"help"          : [],
"process_name"  : "ApplyInletProcess",
"Parameters"    : {
    "model_part_name"  : "AutomaticInlet2D_Inlet",
    "variable_name"    : "VELOCITY",
    "modulus"          : 1.0,
    "direction"        : "automatic_inwards_normal",
    "interval"         : [0,"End"]
}
```

Figure 3: Example of BC in *json* format

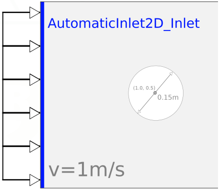

Figure 4: Subm. BC

Other classes

Process

`Process` is the place for adding new algorithms to *Kratos*. Mapping algorithms, Optimization procedures and many other type of algorithms can be implemented as a new process in *Kratos*.

Data containers

`Data containers` A data value container is a heterogeneous container with a variable base interface designed to hold the value for any type of variable

Listing 1: Example using *MMG* **API** in `Process`

```cpp
template<>
void MmgProcess<2>::InitMesh()
{
    mmgMesh = nullptr;
    mmgSol = nullptr;

    // We init the MMG mesh and sol
    MMG2D_Init_mesh(
      MMG5_ARG_start,
      MMG5_ARG_ppMesh,
      &mmgMesh,
      MMG5_ARG_ppMet,
      &mmgSol,
      MMG5_ARG_end);

    InitVerbosity();
}
```

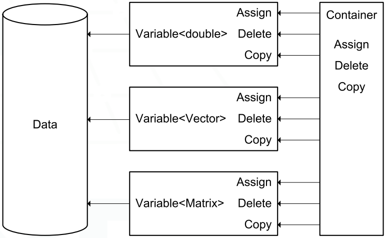

Figure 5: Variable

Section 2

Theory

Level set remeshing

We compute the gradient (1) of a scalar variable f in order to compute an anisotropic metric to remesh, using the procedure from (2)

$$\nabla f = \frac{\partial f}{\partial x}\mathrm{i} + \frac{\partial f}{\partial y}\mathrm{j} + \frac{\partial f}{\partial z}\mathrm{k} \tag{1}$$

Level set metric computation

Calling h the element size and ρ the anisotropic ratio
The scalar value f and ∇f the gradient from that scalar. $\mathcal{M}$ is the metric
We compute the following auxiliar coefficients:

$$\begin{cases} c_0 = \frac{1.0}{h^2} & \text{Isotropic metric} \\ c_1 = \frac{c_0}{2} & \text{Applying anisotropic ratio} \end{cases} \tag{2a}$$

For **2D**:

$$\mathcal{M} = \begin{pmatrix} c_0(1-\nabla f_x^2) + c_1 \nabla f_x^2 & (c_1 - c_0)\nabla f_x \nabla f_y \\ (c_1 - c_0)\nabla f_x \nabla f_y & c_0(1-\nabla f_y^2) + c_1 \nabla f_y^2 \end{pmatrix} \tag{2b}$$

For **3D**:

$$\mathcal{M} = \begin{pmatrix} c_0(1-\nabla f_x^2) + c_1 \nabla f_x^2 & (c_1 - c_0)\nabla f_x \nabla f_y & (c_1 - c_0)\nabla f_x \nabla f_z \\ (c_1 - c_0)\nabla f_x \nabla f_y & c_0(1-\nabla f_y^2) + c_1 \nabla f_y^2 & (c_1 - c_0)\nabla f_y \nabla f_z \\ (c_1 - c_0)\nabla f_x \nabla f_z & (c_1 - c_0)\nabla f_y \nabla f_z & c_0(1-\nabla f_z^2) + c_1 \nabla f_z^2 \end{pmatrix} \tag{2c}$$

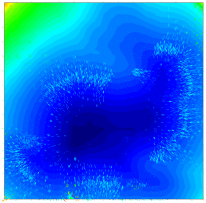

Figure 6: Scalar and its gradient

Hessian remeshing

Following a similar procedure like in the case of the level set, we can compute the hessian matrix (3) of a scalar variable f

$$H = \begin{bmatrix} \frac{\partial^2 f}{\partial x_1^2} & \cdots & \frac{\partial^2 f}{\partial x_1\,\partial x_n} \\ \vdots & \ddots & \vdots \\ \frac{\partial^2 f}{\partial x_n\,\partial x_1} & \cdots & \frac{\partial^2 f}{\partial x_n^2} \end{bmatrix} \text{ or, just: } H_{i,j} = \frac{\partial^2 f}{\partial x_i \partial x_j} \tag{3}$$

Hessian metric computation

Once the *Hessian* matrix has been computed we can compute the corresponding anisotropic metric by the following

$$\mathcal{M} = \mathcal{R}^t \tilde{\Lambda}^t \mathcal{R} \text{ where } \tilde{\Lambda} = (\tilde{\lambda}_i) \text{ being } \tilde{\lambda}_i = \min\left(\max\left(\frac{c_d|\lambda_i|}{\epsilon}, \frac{1}{h_{max}^2}\right), \frac{1}{h_{min}^2}\right) \tag{4a}$$

Being ϵ the error threshold and c_d a constant ratio of a mesh constant and the interpolation ratio
For an isotropic mesh the metric will be:

$$\mathcal{M}_{iso} = diag(\max(\tilde{\lambda}_i)) = \begin{pmatrix} \max(\tilde{\lambda}_i) & 0 & 0 \\ 0 & \max(\tilde{\lambda}_i) & 0 \\ 0 & 0 & \max(\tilde{\lambda}_i) \end{pmatrix} \tag{4b}$$

For anisotropic mesh will be:

$$\mathcal{M}_{aniso} = \mathcal{R}^t \begin{pmatrix} \max(\min(\tilde{\lambda}_1, \tilde{\lambda}_{max}), R_{\lambda rel}) & 0 & 0 \\ 0 & \max(\min(\tilde{\lambda}_2, \tilde{\lambda}_{max}), R_{\lambda rel}) & 0 \\ 0 & 0 & \max(\min(\tilde{\lambda}_3, \tilde{\lambda}_{max}), R_{\lambda rel}) \end{pmatrix} \mathcal{R} \tag{4c}$$

Being $R_{\lambda rel} = |\tilde{\lambda}_{max} - R_\lambda|$ where $R_\lambda = (1-\rho)|\tilde{\lambda}_{max} - \tilde{\lambda}_{min}|$

Metric intersection

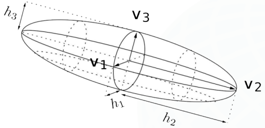

(a) Metric analogy

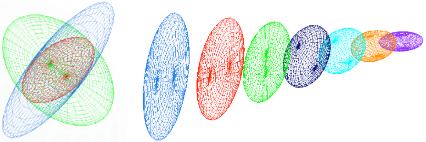

(b) Interpolation

The metric intersection consists in keeping the most restrictive size constraint in all directions imposed by this set of metrics[2]

Procedure

The simultaneous reduction enables to find a common basis such that $\mathcal{M}_1$ and $\mathcal{M}_2$ are congruent to a diagonal matrix, in this basis then $\mathcal{N}$ is introduced

$$\mathcal{N} = \mathcal{M}_1^{-1}\mathcal{M}_2 \text{ considering that can be decomposed in } \lambda_i = \mathrm{e}_i^t \mathcal{M}_1 \mathrm{e}_i \text{ and } \mu_i = \mathrm{e}_i^t \mathcal{M}_2 \mathrm{e}_i \tag{5a}$$

Considering $\mathcal{P} = (\mathrm{e}_1 \mathrm{e}_2 \mathrm{e}_3)$ be the matrix the columns of which are the eigenvectors of $\mathcal{N}$ (common basis)

$$\mathcal{M}_1 = \mathcal{P}^{-t} \begin{pmatrix} \lambda_1 & 0 & 0 \\ 0 & \lambda_2 & 0 \\ 0 & 0 & \lambda_3 \end{pmatrix} \mathcal{P}^{-1} \text{ and } \mathcal{M}_2 = \mathcal{P}^{-t} \begin{pmatrix} \mu_1 & 0 & 0 \\ 0 & \mu_2 & 0 \\ 0 & 0 & \mu_3 \end{pmatrix} \mathcal{P}^{-1} \tag{5b}$$

Computing the metric intersection as:

$$\mathcal{M}_{1\cap 2} = \mathcal{M}_1 \cap \mathcal{M}_2 = \mathcal{P}^{-t} \begin{pmatrix} \max(\lambda_1, \mu_1) & 0 & 0 \\ 0 & \max(\lambda_2, \mu_2) & 0 \\ 0 & 0 & \max(\lambda_3, \mu_3) \end{pmatrix} \mathcal{P}^{-1} \tag{5c}$$

Internal variables transfer

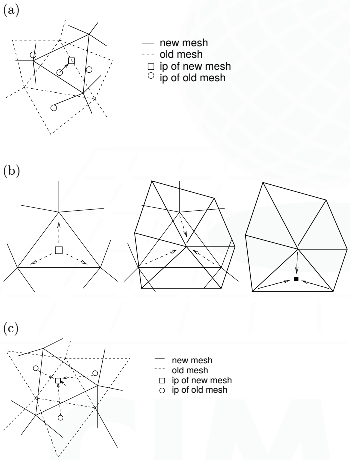

Figure 7: Transfer operators

The Figure 7 shows graphically how each one of the transfer methods work

Techniques

- *CPT*: Closest Point Transfer. **(a)**

  It just takes the value from the closest point

  It provides acceptable results at low cost

- *SFT*: Shape Function Projection transfer. **(b)**

  It interpolates the values using the standard **FEM** shape functions

  Leads to an artificial damage diffusion, but preserves the original shape of the damage profile

- *LST*: Least-Square Projection transfer. **(c)**

  It uses an *least-square* transfer across the closest points

  It is probably the most accurate technique but computationally more expensive

Some example will be shown following

Fundamentals in frictionless contact

The potential corresponding with the frictionless contact is defined in (6a).

$$\mathcal{W}^{co}(\mathrm{u}, \boldsymbol{\lambda}_n) = \int_{\Gamma_c^{(1)}} \boldsymbol{\lambda}_n \cdot \mathrm{g}_n \mathrm{d}A_0 \qquad (6a)$$

We write the gap function as (6b).

$$\mathrm{g}_n = \int_{\Gamma_c^{(1)}} \mathrm{n}^{(1)} \cdot \left(\mathrm{u}^{(1)} - \mathrm{u}^{(2)}\right) \mathrm{d}A_0 \qquad (6b)$$

The normal contact conditions can then be represented as *Karush-Kuhn-Tucker*(**KKT**) (Figure 8) conditions.

$$\begin{cases} g_n \geq 0 \\ p_n \leq 0 \\ p_n g_n = 0 \end{cases} \quad \text{on } \Gamma_c^{(i)} \times [0, T] \qquad (6c)$$

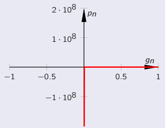

Figure 8: **KKT** condition

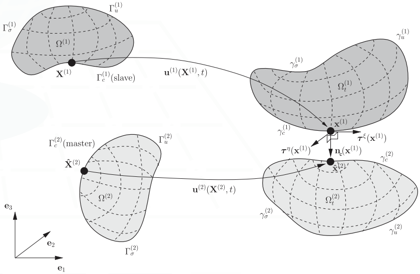

Figure 9: Contact kinematics

ALM Functional

$$\mathcal{W}^{co}(\mathrm{u}, \boldsymbol{\lambda}_n) = \int_{\Gamma_c^{(1)}} k\boldsymbol{\lambda}_n \cdot \mathrm{g}_n + \frac{\varepsilon}{2}\mathrm{g}_n^2 - \frac{1}{2\varepsilon}\langle k\boldsymbol{\lambda}_n + \varepsilon \mathrm{g}_n\rangle^2 \mathrm{d}A_0 \text{ with } \langle x \rangle \begin{cases} x & x \geq 0 \\ 0 & x < 0 \end{cases} \tag{7}$$

Where ε is a positive penalty parameter, k is a positive scale factor

$$\mathcal{W}^{co}(\mathrm{u}, \boldsymbol{\lambda}_n) = \int_{\Gamma_c^{(1)}} \begin{cases} k\boldsymbol{\lambda}_n \cdot \mathrm{g}_n + \frac{\varepsilon}{2}\mathrm{g}_n^2 \mathrm{d}A_0 & \text{if } k\boldsymbol{\lambda}_n + \varepsilon \mathrm{g}_n \leq 0 \text{ (Contact zone)} \\ -\frac{k}{2\varepsilon}\boldsymbol{\lambda}_n^2 & \text{if } k\boldsymbol{\lambda}_n + \varepsilon \mathrm{g}_n > 0 \text{ (Gap zone)} \end{cases} \mathrm{d}A_0 \tag{8}$$

$$\delta\mathcal{W}^{co}(\mathrm{u}, \boldsymbol{\lambda}_n) = \int_{\Gamma_c^{(1)}} \begin{cases} \hat{\boldsymbol{\lambda}}_n \cdot \delta \mathrm{g}_n + k\mathrm{g}_n \delta\boldsymbol{\lambda}_n & \text{if } \hat{\boldsymbol{\lambda}}_n \leq 0 \text{ (Contact zone)} \\ -\frac{k^2}{\varepsilon}\boldsymbol{\lambda}_n \delta\boldsymbol{\lambda}_n & \text{if } \hat{\boldsymbol{\lambda}}_n > 0 \text{ (Gap zone)} \end{cases} \mathrm{d}A_0 \tag{9}$$

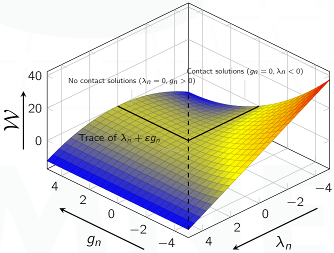

Figure 10: Augmented Lagrangian function for the contact problem

Mortar operators

Definition

Numerical integration of the mortar coupling terms is exclusively performed on the slave side $\Gamma_{c,h}$ of the interface

$$-\delta\mathcal{W}_{co,h} = \sum_{j=1}^{m^{(1)}}\sum_{k=1}^{n^{(1)}} \boldsymbol{\lambda}_{nj}^{T}\left(\int_{\Gamma^{(1)}_{c,h}} \Phi_j N_k^{(1)} \mathrm{d}A_0\right)\delta\mathrm{d}_{nk}^{(1)} - \sum_{j=1}^{m^{(1)}}\sum_{l=1}^{n^{(2)}} \boldsymbol{\lambda}_{nj}^{T}\left(\int_{\Gamma^{(1)}_{c,h}} \Phi_j \left(N_l^{(2)} \circ \chi_h\right) \mathrm{d}A_0\right)\delta\mathrm{d}_{nl}^{(2)} \quad (10)$$

$$\mathrm{D}[j,k] = D_{jk}\mathrm{I}_{ndim} = \int_{\Gamma^{(1)}_{c,h}} \Phi_j N_k^{(1)} \mathrm{d}A_0 \mathrm{I}_{ndim}\ ,\ j = 1,\ldots m^{(1)}\ ,\ k = 1,\ldots n^{(1)} = \boxed{\sum_{g=1}^{ngp} w_g \phi_{gj} N_{gk}^{(1)} J_g^{(1)}} \quad (11a)$$

$$\mathrm{M}[j,l] = M_{jl}\mathrm{I}_{ndim} = \int_{\Gamma^{(1)}_{c,h}} \Phi_j \left(N_l^{(2)} \circ \chi_h\right) \mathrm{d}A_0 \mathrm{I}_{ndim}\ ,\ j = 1,\ldots m^{(1)}\ ,\ k = 1,\ldots n^{(2)} = \boxed{\sum_{g=1}^{ngp} w_g \phi_{gj} N_{gk}^{(2)} J_g^{(1)}} \quad (11b)$$

Derivatives

$$\Delta\mathrm{D}[j,k] = \boxed{\sum_{g=1}^{ngp} w_g \Delta\phi_{gj} N_{gk}^{(1)} J_g^{(1)} + \sum_{g=1}^{ngp} w_g \phi_{gj} \Delta N_{gk}^{(1)} J_g^{(1)} + \sum_{g=1}^{ngp} w_g \phi_{gj} N_{gk}^{(1)} \Delta J_g^{(1)}} \quad (12a)$$

$$\Delta\mathrm{M}[j,l] = \boxed{\sum_{g=1}^{ngp} w_g \Delta\phi_{gj} N_{gk}^{(2)} J_g^{(1)} + \sum_{g=1}^{ngp} w_g \phi_{gj} \Delta N_{gk}^{(2)} J_g^{(1)} + \sum_{g=1}^{ngp} w_g \phi_{gj} N_{gk}^{(2)} \Delta J_g^{(1)}} \quad (12b)$$

Semismooth Newton method

Introduction

Unilateral contact causes one major additional complexity with regard to global solution schemes which divide the set of all discrete constraints into two *a priori* unknown sets of **active** and **inactive** constraints

We re-arrange the **KKT** conditions such that a *Newton–Raphson* type algorithm can be applied

This function in the case of frictionless case basically corresponds with the augmented normal contact pressure

$$\hat{\boldsymbol{\lambda}}_n = k\boldsymbol{\lambda}_n + \varepsilon g_n \begin{cases} \hat{\boldsymbol{\lambda}}_n < 0 \text{ Active} \\ \hat{\boldsymbol{\lambda}}_n \geq 0 \text{ Inactive} \end{cases} \tag{13}$$

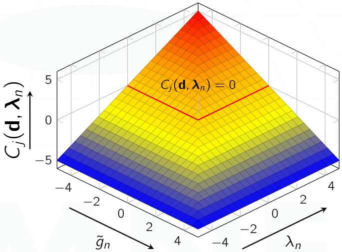

Figure 11: Complementary function of $\hat{\boldsymbol{\lambda}}_n$

Numerical contact remeshing (I)

NOTE: Work of *Anna Rehr* from **TUM**

Error estimation[8]

Residual based methods

- **Internal residual** (r): Error in the differential equation
- **Boundary error** (R):
  - *Traction boundaries*: Difference stress and traction
  - *Interelement boundaries*: Stress jumps
  - *Contact boundary*: Difference stress and contact pressure

$$\|e\|_{E,K} \approx \|\hat{e}\|_{E,K} = C[h_k^2\|r\|_{L_2(K)} + h_K^2\|R\|_{L_2(\partial K)}]$$

- Sound mathematical error bounds
- Determination of the constant C not trivial
- Quality depends heavily on the chosen constant

Recovery based methods

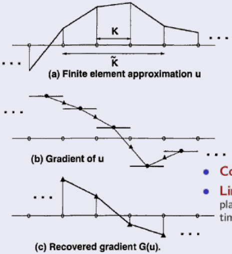

- **Constant stress FE solution**
- **Linear recovered solution:** Replaces the exact solution in the error estimation

$$\|e\|_{E,K} \approx \|\hat{e}\|_{E,K} = \left[\int_{\Omega_K} (\boldsymbol{\sigma}^* - \boldsymbol{\sigma}_h)^T D^{-1} (\boldsymbol{\sigma}^* - \boldsymbol{\sigma}_h)\right]^{\frac{1}{2}} d\Omega_K$$

- Robust
- Easy implementation, no unknown constant, easy extensibility
- No sound mathematical error bounds

Numerical contact remeshing (II)

NOTE: Work of *Anna Rehr* from TUM

The present work introduces a modified version of the **SPR**[8] method

Modified SPR

Element patch:

All elements that are neighboring one node

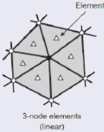

- **Concept**:
  - Stresses at the integration points show superior convergence behavior
  - Use these points to compute the superior stress field
- **Procedure**:
  - Execute a polynomial least square fit with the integration points
  - Compute with this polynomial recovered stress at the center node
  - Compute the stress field by interpolation with the shape functions

Extension for contact mechanics

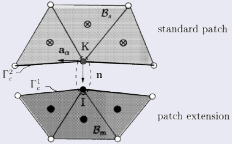

- **Existing approach (penalty formulation)**:
  - Couple patches at the contact boundary
  - Enforce stress continuity in the recovery procedure by a penalty formulation
- **Anna Rehr's work**:
  - Patch coupling not necessary: contact pressure is known (Lagrange Multiplier)
  - Contact BC are regarded in the recovered stress calculation by a penalty formulation which forces the stresses to coincide with the contact pressure

Section 3

Cases

Coarse sphere

In this problem we remesh using the gradient of the distance function, which is the distance to the plane contained in the sphere center.

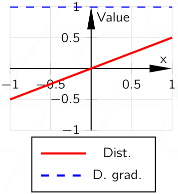

Figure 12: Distance function

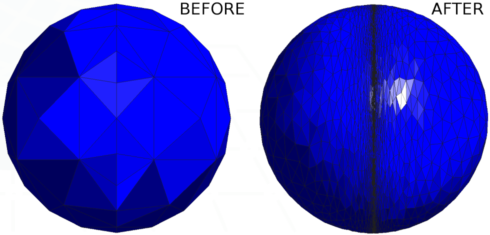

Figure 13: Mesh before and after remeshing

The function can be seen in the Figure12

Stanford's bunny

Geometry of the *Standford*'s bunny[4].

Figure 14: Standford's bunny

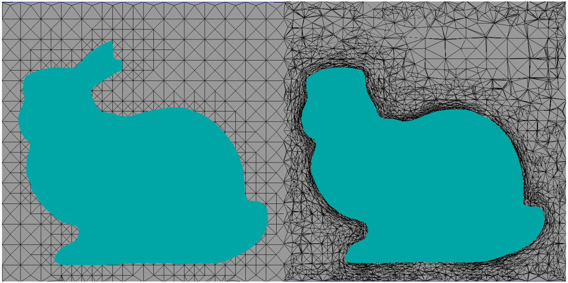

(a) Octree mesh (b) Anisotropic mesh

Figure 15: Mesh before and after remeshing

Anisotropically remesh the geometry using the distance gradient as error measure .
Previously meshed with an embedded octree mesher (*GiD*).

Embedded fluid channel 2D

Adaptative anisotropic remeshing of 2D fluid channel with sphere using as level set the distance function. The problem is solved using an embedded formulation
It consists in a channel 5x1, a sphere of 0.3 diameter and with a velocity of 1 m/s in the inlet an zero pressure in the outlet. The resulting flow has *Reynolds* number of **100**.

(a) Problem

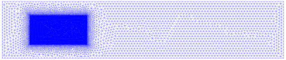

(b) Initial mesh

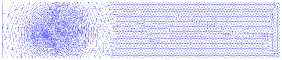

(c) Remeshed

Figure 16: Setup

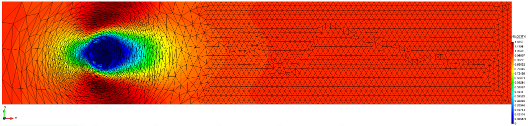

(a) Velocity

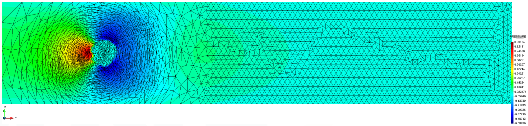

(b) Pressure

Lamborghini

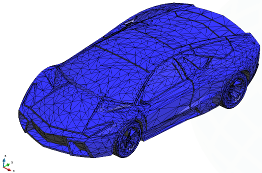

(c) View 1

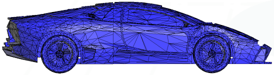

(d) View 2

Figure 17: Lamborghini

In this test case we want to remesh anisotropically the geometry of *Lamborghini*, more complex that the previous bunny.
Anisotropically remesh the geometry using the distance gradient as error measure.
Previously meshed with an embedded octree mesher (*GiD*).

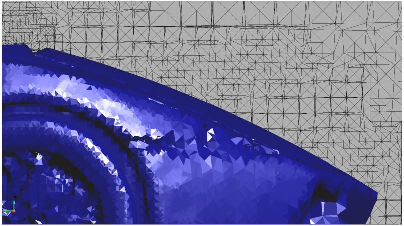

(a) Octree mesh

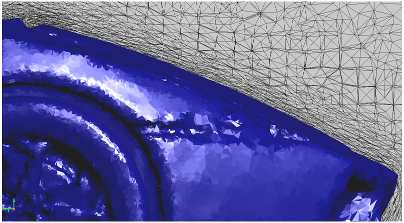

(b) Anisotropic mesh

Figure 18: Mesh before and after remeshing

Hessian 2D

The problem corresponds with the example proposed in reference[2]

The objective is to remesh the structured 1x1 mesh with the error function from Figure 19 and equation (14)

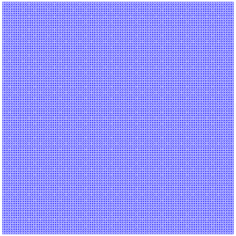

Figure 19: Initial mesh

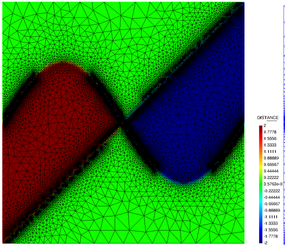

(a) Error estimation

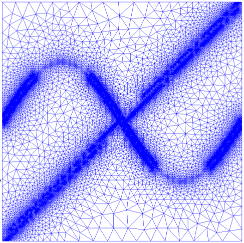

(b) New mesh

Figure 20: Solution

The χ shaped function:

$$f(x, y) = \tanh(-100(y - 0.5 - 0.25\sin(2\pi x))) + \tanh(100(y - x)) \tag{14}$$

Hessian 3D

An extension of the previous problem to 3D in several remeshing iterations

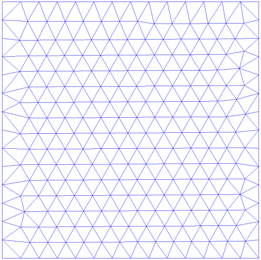

Figure 21: Initial mesh

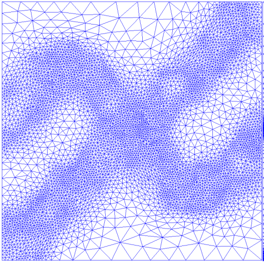

(a) Iteration 1

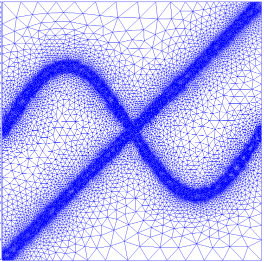

(b) Iteration 2

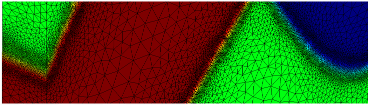

(c) Error estimation

Figure 22: Solution

Beam 2D

The simulation considers 100 time steps of 0.01s. The problem will be remeshed each ten steps considering the Hessian of the displacement

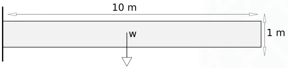

(a) Problem

(b) Initial mesh

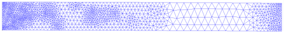

(c) Mesh 1

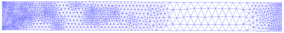

(d) Mesh 2

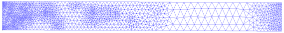

(e) Mesh 3

Figure 23: Setup

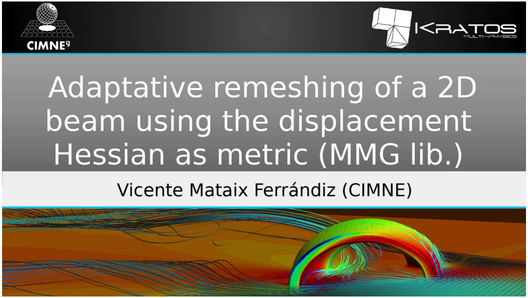

Fluid channel 2D

Adaptative remeshing of 2D fluid channel with sphere using Hessian of velocity as metric measure. It consists in a channel 3x1, a sphere of 0.5 diameter and with a velocity of 1 m/s in the inlet an zero pressure in the outlet.

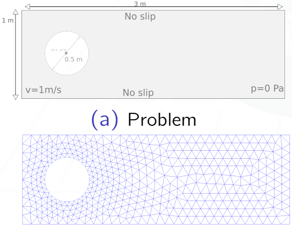

(a) Problem

(b) Initial mesh

Figure 24: Setup

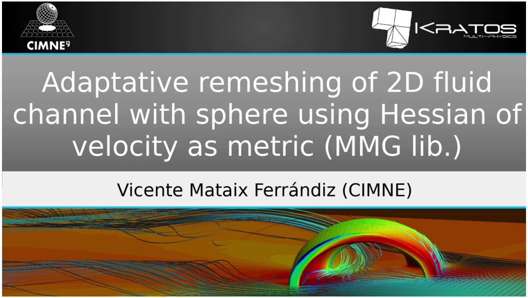

Fluid channel 3D

Adaptative remeshing of 3D fluid channel with sphere using Hessian of velocity as metric measure. It consists in a channel 3x1x1, a sphere of 0.5 diameter and with a velocity of 1 m/s in the inlet an zero pressure in the outlet.

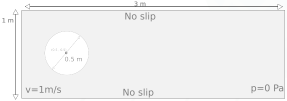

(a) Problem

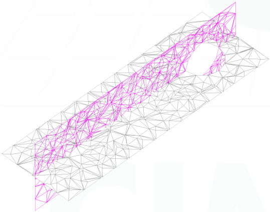

(b) Initial mesh

Figure 25: Setup

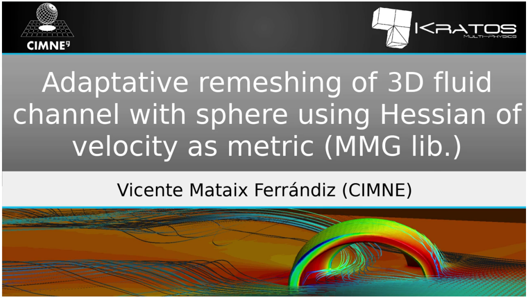

Beam 2D

The simulation considers 10 time steps of 0.01s
The problem will be remeshed each ten steps considering the Hessian of the displacement
A J2-plasticity law has been considered

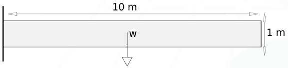

(a) Problem


(b) Initial mesh

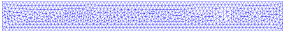
(c) After remeshing

Figure 26: Setup

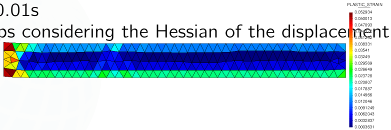

(a) Initial mesh

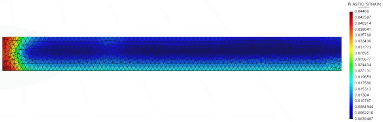

(b) LST

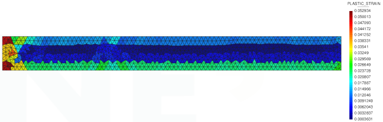

(c) CPT

Patch test

NOTE: Work of *Anna Rehr* from **TUM**

The patch test is the most absic test to pass to verify a contact formulation
It has been solved in 2D using the modification of the **SPR**

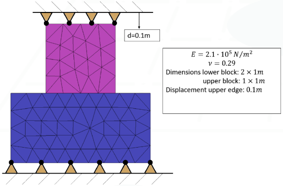

Figure 27: Setup

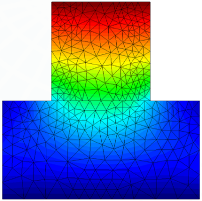

Iteration 1, error estimation based on standard SPR

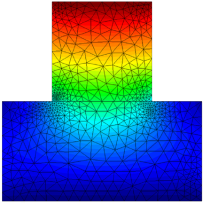

Iteration 2, error estimation based on standard SPR

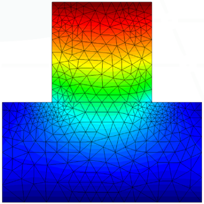

Iteration 1, error estimation based on SPR with contact extension

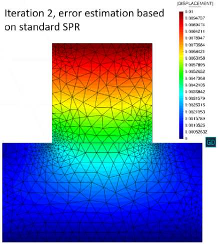

Iteration 2, error estimation based on SPR with contact extension

Figure 28: Solution

Hertz problem

NOTE: Work of *Anna Rehr* from **TUM**

The *Hertz* test is a very used benchmark for contact mechanics
It has been solved both in 2D and 3D using the modification of the **SPR**

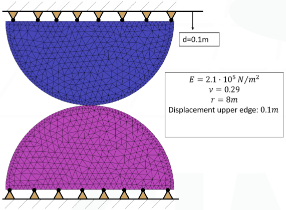

Figure 29: Setup

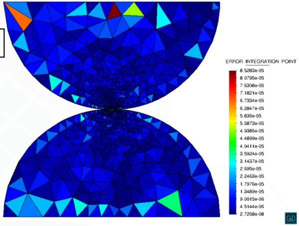

(a) Error

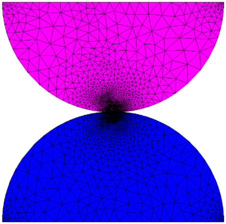

(b) Final mesh 2D

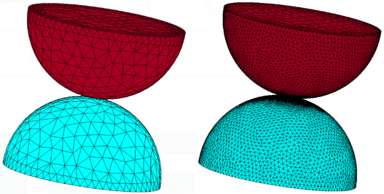

(c) Final mesh 3D

Section 4

Conclusions

Problematic on implementation

During the integration of *MMG* we have some problems, like the following:

Problems

- **Some bugs in the creation of new geometries**: Ghost geometries appeared some times
- **Submodelparts integration**: The nodes are problematic (can belong to several geometries at the same time)
- **Some processors give problems**: Some flags of optimization are removed in order get things to work
- **Tensor notation**: Notation are always problematic

Thanks for the fast reply in the *MMG* forum!!

Conclusions and future work

Conclusions

- *MMG:* We have implemented into *Kratos* the *MMG* **API**
- *Metrics*: We have implemented several metric measures and utilities
- *Internal values*: We have implemented several utilities in order to interpolate internal values
- *Contact*: We have implemented an extended version of **SPR** in order to be able to compute contact remeshing

Future works

- *New problems*: Use the process for new problems not computed yet (for example *FSI*)
- *Contact*: Improve the contact remeshing implementation
- *Extend*: Extend the *Kratos*/*MMG* integration

Visit us at GitHub

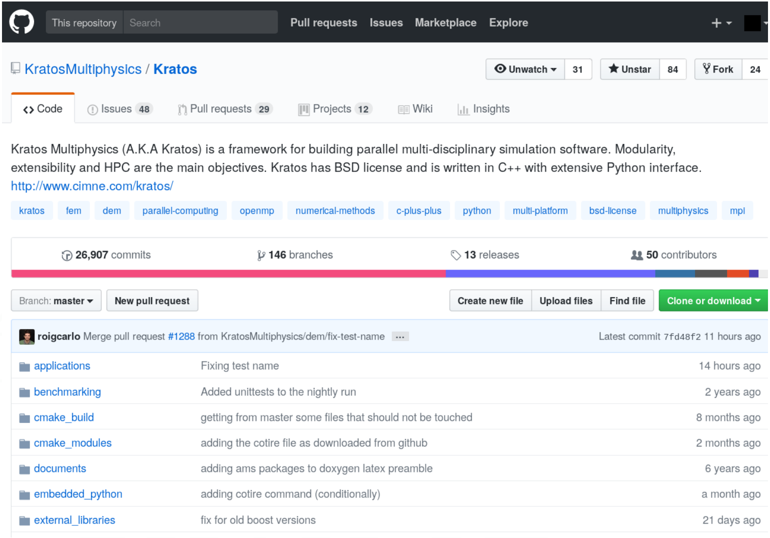

Figure 30: https://github.com/KratosMultiphysics/Kratos

Many thanks

(a) International Center for Numerical Methods in Engineering

(b) Chair of Structural Analysis Technical University of Munich

Figure 31: Main contributors

(a) Airbus Defence and Space Stress Methods Department

(b) Siemens AG Corporate Optimisation Technology

(c) ONERA, The French Aerospace Lab Applied Aerodynamics Department

Figure 32: Known Users

And many thanks to our community!!

References

- *P. Dadvand, R. Rossi, E. Oñate*: *An Object-oriented Environment for Developing Finite Element Codes for Multi-disciplinary Applications.* Computational Methods in Engineering. 2010
- *F. Alauzet*: *Metric-Based Anisotropic Mesh Adaptation.* Course material, CEA-EDF-INRIA Schools. Numerical Analysis Summer School. 2007
- *P. Tremblay*: *2-D, 3-D and 4-D Anisotropic Mesh Adaptation for the Time-Continuous Space-Time Finite Element Method with Applications to the Incompressible Navier-Stokes Equations.* PhD thesis Ottawa-Carleton Institute for Mechanical and Aerospace Engineering, Department of Mechanical Engineering, University of Ottawa. 2007
- *G.Turk, M. Levoy*: *The Stanford 3D Scanning Repository.*
- *P.J. Frey, F. Alauzet*: *Anisotropic mesh adaptation for CFD computations.* Comput. Methods Appl. Mech. 2004
- *P.J. Frey, F. Alauzet*: *Anisotropic mesh adaptation for transient flows simulations*
- *M. Bellet*: *Adaptive mesh technique for thermal–metallurgical numerical simulation of arc welding processes*, International Journal for Numerical Methods in Engineering, 2008.
- *Zienkiewicz, O. C. and Zhu, J.Z. and Taylor, Robert L.*: *The Finite Element Method: its Basis and Fundamentals*, Butterworth-Heinemann, 2013.
- *P.J. Frey, F. Alauzet*: *Estimateur d'erreur geometrique et metriques anisotropes pour l'adaptation de maillage. Partie I : aspects theoriques*, HAL Id: inria-00071827, 2006

Thank you very much for your attention